Journal of Applied Research and Technology

www.jart.icat.unam.mx

Journal of Applied Research and Technology 22 (2024) 9-21

Original

Energy harvesting system using broadband textile antennas

J. Porras[a]* • A. Acosta[a] • A. Corona[a] • G. Puerto[b]

[a]*Instituto de Astrofísica, Óptica y Electrónica, San Andrés de Cholula, México*
[b]*Universidad Distrital Francisco José de Caldas, Bogotá, Colombia*

Received 04 27 2022; accepted 11 25 2022
Available 02 29 2024

Abstract: Taking advantage of the benefits provided by the energy harvesting from ambient radio frequency sources, a multi-band receiver is designed and manufactured using broadband antennas constructed with textile materials to be adapted into a T-shirt. The antennas connected to the rectifier allow to capture energy from the environment from four mobile bands: 1700, 1800, 1900 and 2100 MHz, and from the 2400 MHz WiFi band.

Keywords: Rectenna, energy harvesting, textile antenna, wearable antenna, multiband rectifier

*Corresponding author.
E-mail address: jhporrasd@correo.udistrital.edu.co (J. Porras).
Peer Review under the responsibility of Universidad Nacional Autónoma de México.

1. Introduction

Energy harvesting is the process by which the energy derived from environment sources, such as: solar, wind, kinetic energy and energy derived from electromagnetic waves is captured and used to power electronic devices. Currently, the energy coming from radiofrequency signals from mobile phones, base stations, television, etc., provide a wide electromagnetic spectrum to collect energy (Jabbar et al., 2010).

Thanks to new advances in low power electronics, radio frequency (RF) energy harvesting from the environment has increased its viability as power source for small electronic devices. Unlike the energy coming from the sun, it is possible to work at night and inside buildings, furthermore the antennas already implemented in smartphones and network devices can be used to recollect energy without making changes to the device (Agilent Technologies, 2005).

To date, several approaches have been proposed to RF energy harvesting. In the paper of Naresh et al. (2017), a prototype to collect energy from radio frequency signals using a 2-stage half-wave rectifier, designed with Schottky detector diodes to work at 2.45 and 5.8 GHz was proposed. A maximum efficiency of 60% and a voltage of 0.82 V output when the input power is 0 dBm was achieved. On the other hand, they build a microstrip antenna using cotton jean as a substrate to work from 2.2 to 3.3 GHz and from 4.0 to 6.73 GHz. The maximum gain achieved with these antennas was 3.5 dBi. Also, a 1-stage rectifier using Schottky diodes to work at 2.45 GHz, achieving a maximum efficiency of 65% at -2 dBm and a microstrip antenna manufactured using felt, polyester and copper cloth to work between 2.4 and 2.5 GHz, achieving a maximum gain of 8.1 dBi and an efficiency of up to 73% is presented in the paper of Adami et al. (2018). On the other hand, Borges et al. (2014) Manufactured a 5-stage Dickson rectifier that worked at 900 and 1800 MHz, achieving a maximum efficiency of 36% and an output voltage of 4.67 V when the input power is 0 dBm. Cordura fabric and zelt fabric were used as substrate for the manufacture of the antenna; designed to work from 820 to 1000 MHz and from 1690 to 1930 MHz, achieving a maximum efficiency of 82% and a maximum gain of 2.1 dBi.

This paper presents the design and implementation of a rectenna capable of working in multiple frequency bands, with the purpose of obtaining a better use of the energy present in the environment. It is important to mention that the work focuses on the construction of a prototype, which, unlike most of the works found in the literature is implemented in a common T shirt.

This paper is organized as follows: In section 2, a multi-band rectifier is designed and simulated to work with signals of different frequency bands. Section 3 covers the design and simulation of two broadband microstrip antennas to be implemented in clothing. Section 4 presents the physical results of the rectifier, antennas, and the system in operation. Section 5 summarizes the conclusions of this work.

2. Multiband Rectifier

Due to the very low power of the RF signals present in the environment, it is necessary to design a rectifier capable to pick up signals of the order of the microwatts. Therefore, it is helpful if the device works in the frequencies where there is more energy, such as the Mobile Networks Global System for Mobile Communication (GSM), Long Term Evolution (LTE) and the Industrial, Scientific and Medical band (ISM). In addition, voltage multipliers are required due to the low voltage of the signals.

2.1. Diode selection

The diode must work with high frequency and very low power signals, so its power consumption must be very low. Schottky diodes are the best choice for fast switching and very low threshold voltages (de la Peña & del Castillo, 2009). The HSMS-285x family of zero bias Schottky detector diodes are the most widely used in RF energy harvesting applications due to its good performance. These diodes are manufactured to work with powers below -20 dBm and provide good performance at frequencies lower than 1.5 GHz; they even can operate at higher frequencies with a reduced performance (Mutee-Ur-Rehman et al., 2017).

2.2. Rectifier topology

A rectifier-multiplier is designed to work in four frequency bands. For this purpose, a circuit consisting of two opposite Cockcroft-Walton cells is used as seen in Figure 1, which allows full wave rectification, a small ripple voltage and a more continuous output signal. A voltage quadrupler can be observed in Figure 1, the reason for choosing this multiplication factor and not a greater one is because for each added diode the losses increase.

Where V_p and V_d are the source and diode voltages. Capacitors are chosen in such a way that they produce a low ripple voltage, however it is difficult to get large capacitances to work at high frequencies, so 10 pF is used. An output resistance of 12 KΩ is chosen for the highest efficiency.

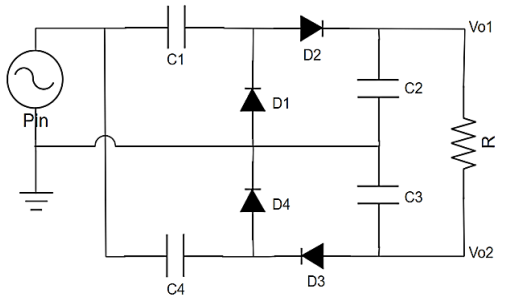

Figure 1. Full wave rectifier.

The circuit output voltage equation is as follows:

$$V_o = V_{o1} - V_{o2} = 4(V_p - V_d) \quad (1)$$

2.3. Rectifier implemented using lumped elements

The coupling circuit consists of inductors placed in series with the diodes to eliminate the capacitive reactance at the frequencies of interest as shown in Figure 2. This coupling network provides a wide bandwidth and requires few components for its implementation.

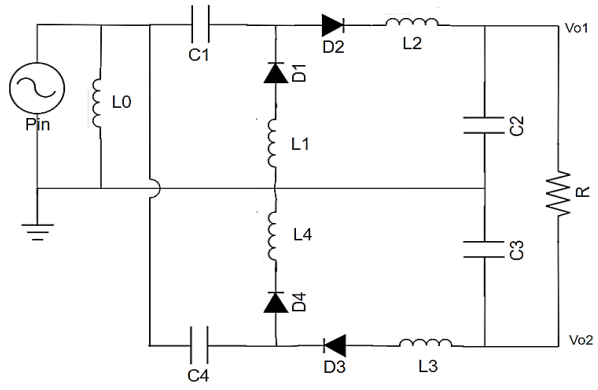

Figure 2. Coupling circuit to achieve four bands operation.

For the design, four mobile phone bands are chosen: 1700, 1800, 1900 and 2100 MHz, and the WiFi band of 2400 MHz. For the sake of calculating the value of the inductances (L_1, L_2, L_3, L_4), the input impedance of the rectifier (Z_{in}) must be obtained and set equal to 0; next step is to calculate the inductance from the equation. For this, only the imaginary part of Z_{in} is considered.

2.3.1. Inductance calculation for coupling

The first step is to calculate L_1 for coupling at f=1.75 GHz, not including the inductors L_2, L_3, L_4:

$$L_1 = \frac{X_{L1}}{j\omega_1} = \frac{X_{L1}}{j(2\pi * 1.75 * 10^9)} \quad (2)$$

$$Z_{in} = \{[Z_{D4} \,||\, (Z_{D3} + X_{C3})] + X_{C4}\} \,||\, \{[(Z_{D2} + X_{C2}) || (Z_{D1} + X_{L1})] + X_{C1}\} \quad (3)$$

$$X_c = \frac{1}{j\omega C} = \frac{1}{2\pi(1.75 * 10^9)(10 * 10^{-12})} = -9.1j\Omega \quad (4)$$

Where Z_D is the impedance of the diode, X_C and X_L are the capacitor and inductor reactance, respectively.

The diode impedance can be calculated from the equivalent model of the device or by simulation in the software Advanced Design System (ADS). The capacitive reactance of the diode at this frequency is as follows:

$$Z_{D1} = Z_{D3} = -292.25j\Omega \quad (5)$$

$$Z_{D2} = Z_{D4} = -331.5j\Omega \quad (6)$$

Then the imaginary part of Z_{in} is set equal to 0, replace the previous values in the equation and isolate X_{L1} to obtain L_1:

$$L_1 = 27.4\ nH \quad (7)$$

For the coupling at 1.95 GHz, the same procedure used to calculate L_1, is used, this time including L_4 and L_1 in the circuit.

$$Z_{in} = \{[Z_{D4} + X_{L4} \,||\, (Z_{D3} + X_{C3})] + X_{C4}\} \,||\, \{[(Z_{D2} + X_{C2}) || (Z_{D1} + X_{L1})] + X_{C1}\} \quad (8)$$

$$Z_{D1} = Z_{D3} = -258.75j\Omega \quad (9)$$

$$Z_{D2} = Z_{D4} = -293.65j\Omega \quad (10)$$

$$L_4 = 24.6\ nH \quad (11)$$

For the coupling at 2.15 GHz, the same previous procedure is performed, including this time the inductances L_4, L_1 y L_2 in the circuit, obtaining $L_2 = 20.5\ nH$. Finally, for the coupling at f = 2.45 GHz, all the inductances of the circuit are included and $L_3 = 12.5\ nH$ is obtained.

2.3.2. Simulation

By simulating the circuit with the previously calculated values, the return losses presented in Figure 3 were obtained, resulting in the following working frequencies: 1.78 GHz, 2 GHz, 2.2 GHZ and 2.45 GHz. The frequency shift is because of the addition of each inductor affects the previous calculation; this can be corrected by performing multiple iterations to recalculate the inductances.

Through the reflection coefficient, commonly known as parameter S_{11}, it allows to measure the amount of power that is reflected in the input port in comparison with the amount of power that is applied from the power source, which is also known as return loss term.

It is important to highlight that the circuit is optimized by means of simulation so that it covers the mobile bands: 1700, 1800, 1900, 2100 MHz and the Wi-Fi band: 2450 MHz, guaran-

guaranteeing that return losses are less than -10 dB throughout this mentioned frequency range. In this way, the impedance matching is improved adding an inductor L_0 to the input of the rectifier in order to set the real part of Z_{in} to 50 Ω. The final values of the rectifier components are: $L_0 = 6.5$ nH, $L_1 = 27.7$ nH, $L_2 = 18$ nH, $L_3 = 12.5$ nH, $L_4 = 24$ nH. The return loss of the optimized circuit using the previous values is shown in Figure 3.

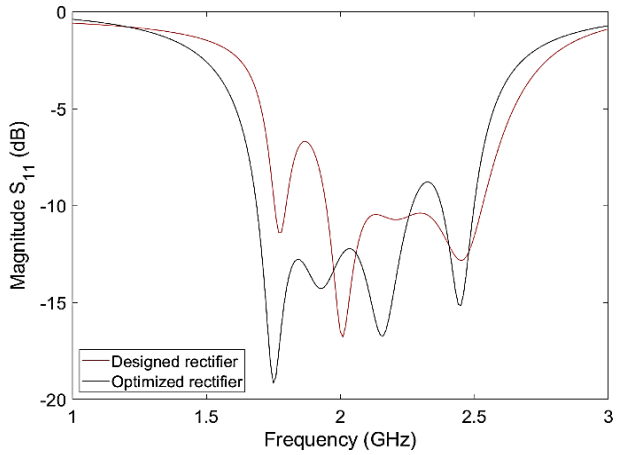

Figure 3. Return loss of the rectifier designed and optimized.

The reflection coefficient simulation result shows that the optimized rectifier improves the response at the design frequencies and bandwidth, covering from 1.69 GHz to 2.26 GHz and from 2.38 GHZ to 2.5 GHz (below -10 dB). The performance of the rectifier is evaluated using the power conversion efficiency equation:

$$\eta = \frac{P_{Occ}}{P_{in}} = \frac{V_{Occ}^2/R}{P_{in}} \quad (12)$$

Where $P_{O_{CC}}$ and P_{in} are the output and input power, respectively. $V_{O_{CC}}$ is the output voltage and R the resistance.

Table 1 shows that the maximum efficiency is slightly above 50% for almost all design frequencies, which occurs when the input power is 0 dBm.

Table 1. Optimized rectifier efficiency.

Frequency (GHz)	Maximum efficiency (%)	Efficiency using Pin=-10 dBm (%)
1.75	46.8	36.4
1.85	54.6	40.0
1.95	61.7	40.1
2.15	51.7	35.2
2.45	51.3	30.6

2.4. Rectifier implemented using distributed elements

There are many advantages when circuits are implemented using transmission lines compared to circuits built using lumped elements. The first reason that we can mention is the facility to manufacture circuits with distributed elements, since it is not necessary to weld inductors and capacitors, furthermore, in this way we avoid welding losses. On the other hand, getting commercial high-frequency capacitors and inductors is not easy, which makes it difficult to build the circuits. Other advantage that we can mention is that transmission lines allow to create more compact circuits and this is very important if we want to implement the prototype in clothes, since we can print the entire circuit on a t-shirt using only transmission lines. The last benefit we can highlight, is that the manufacturing of a circuit using distributed elements is cheaper than a circuit with lumped elements, this is important if the product is to be marketed.

The design is based on the circuit of Figure 2 and it is developed through equivalent conversions between lumped and distributed elements. In the previous section, the rectifier was designed using lumped elements.

2.4.1. Converting concentrated to distributed elements

One of the problems to perform the same circuit using distributed elements is the dependence of the inductance and capacitance with the frequency, for this reason the design is carried out at a specific frequency. This fact causes the bandwidth to decrease dramatically compared to the ideal circuit. The equivalent of a series inductance is a series of transmission lines with an electrical length shorter than 45° and a characteristic impedance modelled in equation (13) (Rhea, 1994).

$$Z_o = \frac{x_L}{\text{sen}(\Theta)} \quad (13)$$

$$\Theta = \beta l = \frac{2\pi}{\lambda} l \quad (14)$$

Where Θ is the electrical length, β is the phase constant, l is the physical length and λ is the wavelength.

The characteristic impedance of a microstrip transmission line is calculated with equation (15) if $W/h < 1$ or with equation (16) if $W/h > 1$ (Balanis, 2016).

$$Z_o = \frac{60}{\sqrt{\varepsilon_{reff}}} ln\left(\frac{8h}{W} + \frac{W}{4h}\right) \quad (15)$$

$$= \frac{\frac{Z_o}{120\pi}}{\sqrt{\varepsilon_{reff}} * \left[\frac{W}{h} + 1.393 + 0.667 \ln\left(\frac{W}{h} + 1.44\right)\right]} \quad (16)$$

Where $\mathcal{E}_{reff}$ is the effective dielectric constant, W is the line width and h the substrate height.

For a grounded inductor, the equivalent is a short circuit terminated line with an electrical length shorter than 90° and a characteristic impedance given by equation (17) (Rhea, 1994).

$$Z_o = \frac{x_L}{\tan(\Theta)} \tag{17}$$

A simple way to obtain large inductance is using a spiral inductor, since the inductance is proportional to the number of turns. Therefore, it is used to couple at the frequencies of 1.75 GHz and 1.95 GHz. The circuit is implemented in a ROGER 5870 substrate, since it has a very low loss tangent; its properties are: $\mathcal{E}_r = 2.33,\ tan\delta = 0.0005\ to\ 0.0012,\ h = 0.79\ mm$ (Rogers Corporation, 2018). The cables connecting the components to the ground plane behave like inductors at high frequencies. The inductance of a cylindrical conductor is as follows (Predella et al., 1991):

$$L = 2\left\{ln\left(\frac{2l}{r}\right) - 0.75\right\}\ nH \tag{18}$$

Where l is the length of the cable and r is the radius.

2.4.2. Simulation

The equivalent rectifier layout obtained using conversions between lumped and distributed elements is shown in Figure 4, and Figure 5 shows the return losses of both the simulated circuits. To physically implement the layout, the dimensions of the diodes (2 mm x 2.1 mm), the width of their pins (0.27 mm) and the size of the capacitors (1.6 mm x 0.81 mm) must be considered. Therefore, the designed transmission lines must be divided into multiple parts that require different line widths, in such a way as to not greatly alter the equivalent inductance.

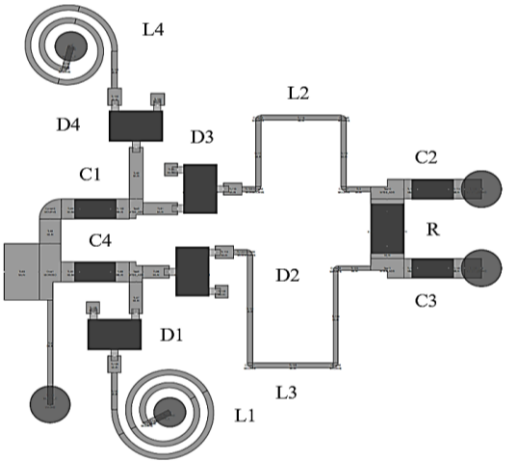

Figure 4. Final rectifier layout.

Table 2. Efficiency results of the final rectifier.

Frequency (GHz)	Maximum efficiency (%)	Efficiency using Pin=-10 dBm (%)
1.75	37.1	23.9
1.85	46.4	25.2
1.95	50.4	21.7
2.15	45.2	20.8
2.45	41.7	14.9

From Figure 5, the bandwidth ranges from 1.71 GHz to 1.97 GHz, covering the 1700 MHz, 1800 MHz and 1900 MHz bands. For the 2100 MHz band it ranges from 2.12 GHz to 2.19 GHz and for the WiFi band from 2.38 GHz to 2.51 GHz.

On other hand, the efficiency results are shown in Table 2 and the decrease in efficiency is due to the dielectric, conduction and radiation losses.

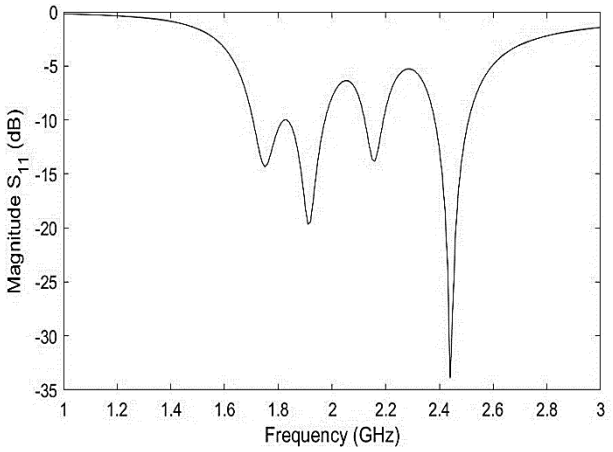

Figure 5. Return loss of the rectifier layout.

3. Textile Antenna

Textiles have a low dielectric constant because they are very porous and the presence of air in them makes the electrical permittivity to be close to 1 as seen in Table 3 (Salvado et al., 2012).

Felt is chosen as substrate because it has a low $\mathcal{E}$r, which allows a better bandwidth, gain and efficiency. This material is very economical compared to many textiles and due to its thickness, it improves the properties of the antenna. Another important material is the conductive fabric (electro textile) used for the patch and the ground plane. These fabrics are based on a copper coated nylon fabric, so they have a high conductivity, but is lower than pure copper that reduces efficiency and gain. Table 4 summarizes the electrical parameters of some conductive textiles.

Table 3. Properties of non-conductive fabrics (Cicchetti et al., 2017; Ouyang & Chappell, 2008; Salvado et al., 2012)

Non-conductive fabric	ε_r	tanδ
Cordura	1.9	0.0098
Cotton	1.6	0.04
100% Polyester	1.9	0.0045
Felt	1.22	0.016
Denim	1.6	0.05
Wool	1.17	0.0035
Quartz	1.95	0,0004
Silk	1.75	0.012
Foamy	1.24	0.0213
Leather	2.72	0.02
Flannel	1.7	0.025

Table 4. Properties of conductive textiles (Cicchetti et al., 2017).

Conductive material	Resistance (Ω/sq)	Conductivity (S/m)	Thickness (mm)
Flectron	0.07	$0.79 * 10^5$	0.18
Shieldit Super	0.05	$1.18 * 10^5$	0.17
Shieldex Nora	0.03	$3.33 * 10^5$	0.1
Zelt	0.01	$16.67 * 10^5$	0.06
Copper Taffeta	0.05	$2.5 * 10^5$	0.035
Copper tape	0.0005	$571 * 10^5$	0.08

3.1. Analysis of a rectangular patch antenna

Since some waves propagate through the substrate and others through the air, the effective dielectric constant is modelled in equation (19) (Balanis, 2016):

$$\varepsilon_{reff} = \frac{\varepsilon_r + 1}{2} + \frac{\varepsilon_r - 1}{2}\left(1 + 12\frac{h}{W}\right)^{-\frac{1}{2}} \quad (19)$$

Where ε_r is the dielectric constant.

Due to field overflow effect, the length of the patch extends a distance ΔL (Balanis, 2016).

$$\frac{\Delta L}{h} = \frac{0.412\left((\varepsilon_{reff} + 0.3)\left(\frac{W}{h} + 0.264\right)\right)}{(\varepsilon_{reff} - 0.258)(\frac{W}{h} + 0.8)} \quad (20)$$

$$L_{eff} = \frac{c}{2f_r\sqrt{\varepsilon_{reff}}} \quad (21)$$

$$L_{patch} = L_{eff} - 2\Delta L \quad (22)$$

Where L_{patch} is the patch length and L_{eff} is the effective length.

The input impedance of the patch in given by equation (23) (Balanis, 2016):

$$Z_{patch} = \frac{1}{2G_1} \quad (23)$$

$$G_1 = \frac{1}{90}\left(\frac{W}{\lambda}\right)^2 \quad (24)$$

Where G_1 is the conductance.

For impedance matching between the source and the patch, a λ/4 transformer is required (Balanis, 2016):

$$L_{acop} = \frac{\lambda}{4} = \frac{c}{4\sqrt{\varepsilon_r}f} \quad (25)$$

$$Z_{acop} = \sqrt{Z_{patch} * Z_o} \quad (26)$$

Where c is the speed of light and f is the frequency.

3.2. Characterization of the material

The felt selected is 2.5 mm thick and according to what was reported in other studies, the dielectric constant is 1.22 and the loss tangent is 0.016 as shown in Table 3. To obtain the electrical permittivity of the material, microstrip antennas are designed and constructed using the model presented in section *3.1*. By means of a Vector Network Analyzer, the parameter S_{11} of the antenna is obtained to identify the resonant frequency; this data is used in the High Frequency Structure Simulator (HFSS) to obtain the dielectric constant that produces this frequency. Finally, the results are averaged and an electrical permittivity of 1.12 was obtained, which is consistent with previous studies.

3.3. Broadband Antenna based on rectangular patches

The geometry of these antennas is optimized until achieving the best performance. The first modification made to the rectangular patch antenna is to modify the ground plane geometry to increase impedance bandwidth. The next modification is to cut the sides of the patch to achieve smooth changes in the impedance response S_{11}. Finally, a cut is made in the ground plane below the coupling line and a copper tape is added at the back as shown in Figure 6.

Based on the antenna design in the previous section, Figure 7 shows the array of two elements fed in parallel in order to increase the gain. The array consists of only two elements due to the large size of the prototype. The calculations for the coupling line are made at the center frequency between 1.7 GHz and 2.5 GHz (2.1GHz). A W = 50 mm is used for the patch (width of copper tape). The transmission lines connecting the patches to the feeding line are 100 Ω; the impedance is divided by 2 at the intersection (feeding line).

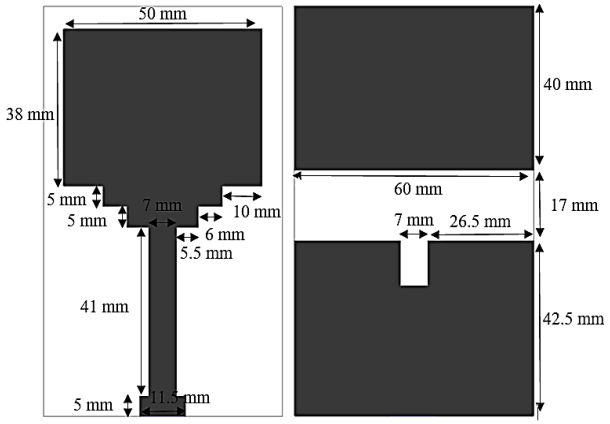

Figure 6. Simulated antenna. Front and rear view.

3.4. Antenna array based on two rectangular patches

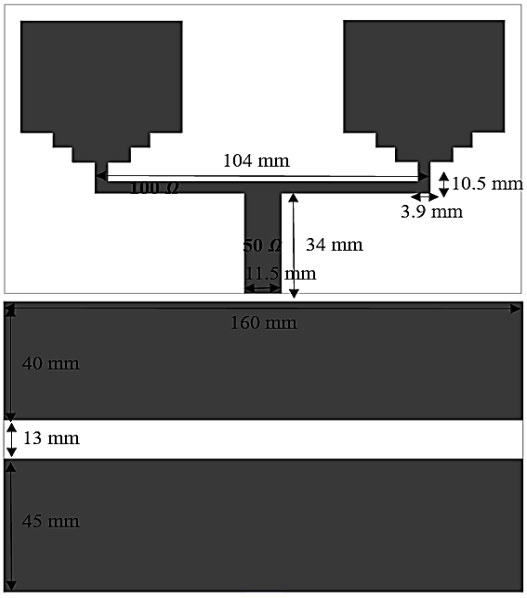

Figure 7. Top and rear view of antenna array.

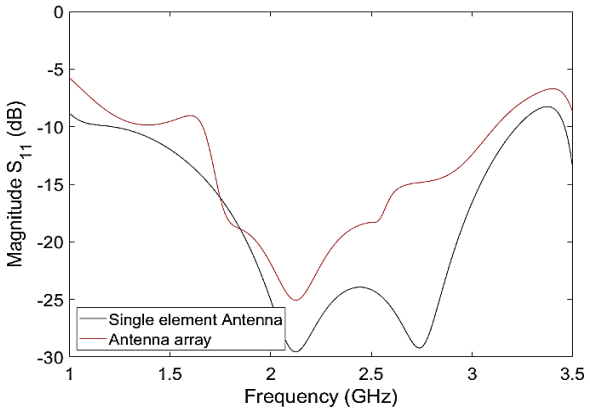

Figure 8. Return loss of 1 and 2 element antennas.

Both, the single element and array antenna reflection coefficient (S_{11} < -10 dB) is shown in Figure 8. The single element bandwidth ranges from 1100 to 3200 MHz. The fractional bandwidth is obtained with the following equation:

$$FBW = \frac{f_2 - f_1}{\frac{f_2 + f_1}{2}} . 100 = \frac{3200 - 1100}{\frac{3200 + 1100}{2}} . 100 = 97\% \quad (27)$$

Where f_2 and f_1 are the upper and lower frequency.

The two-element antenna bandwidth ranges from 1670 MHz to 3110 MHz, which corresponds a fractional bandwidth of 65%.

Table 5. Antennas gain with one and two elements.

Freq. (GHz)	1 antenna element gain (dBi)	2 antenna element gain (dBi)	Difference (dB)
1.75	3.6	6.0	2.4
1.85	3.8	6.5	2.7
1.95	4.1	6.7	2.6
2.15	4.5	6.4	1.9
2.45	5.1	5.6	0.5

Table 5 shows the gain at different frequencies for one and two antenna elements and the achieved radiation efficiency is between 91% and 96% for the frequencies of interest.

3.5. Broadband collinear antenna

A series-fed array of rectangular patches known as a collinear antenna is implemented. These antennas are characterized by having a high gain and narrow bandwidth. The elements must be powered in phase, so they are separated by a distance of $\lambda/2$. To increase the bandwidth, the ground plane is appropriately designed (Polivka & Holub, 2007). Figure 9 shows the designed antenna and Figure 10 shows that the bandwidth covers from 1720 MHz to 3370 MHz with a fractional bandwidth of 60%. Table 6 shows the antenna gain results. The radiation efficiency obtained is between 77% and 90% at the frequencies of interest.

4. Experimental Results

4.1. Rectifier

The device was fabricated using a 0.79mm thick ROGER 5870 substrate, and including 4 HSMS-285B diodes, 4x10 pF surface mount RF capacitors (Ref: 6035k100J), a 12 kΩ surface mount resistor (Ref: SMD0805) and a 50 Ω SMA connector. The size of the implemented rectifier is 3.2cm x 2.1cm as shown in Figure 11.

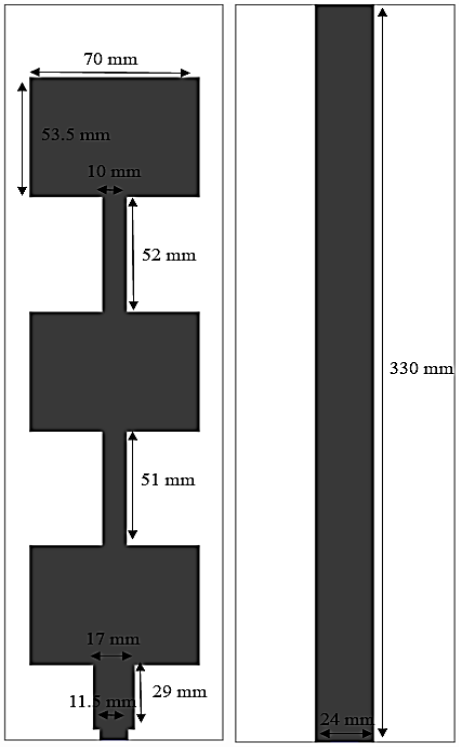

Figure 9. Collinear broadband antenna. Front and rear view.

Table 6. Collinear antenna gain.

Frequency (GHz)	Gain (dBi)
1.75	8.9
1.85	8.6
1.95	8.6
2.15	9.2
2.45	10.04

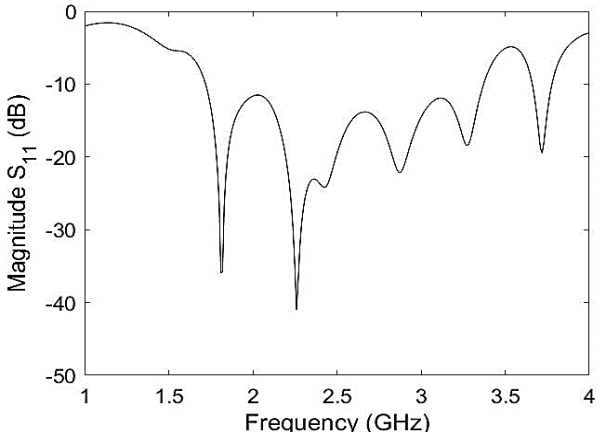

Figure 10. Return loss of the collinear antenna.

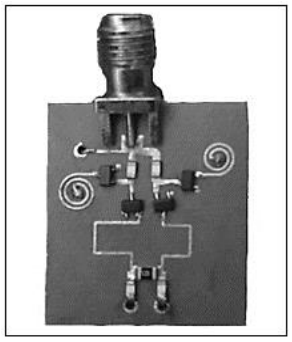

Figure 11. Physical implementation of the rectifier.

From the reflection coefficient shown in Figure 12, it can be observed that the built rectifier has a better coupling with higher input powers. On the other hand, for the first and second frequency band good results were obtained, whereas the third band exhibits the worst case, since the center frequency was significantly shifted and the coupling was not good either (-7dB to -8dB). For the fourth band, only a bandwidth of 30 MHz below -10 dB was achieved, these results are summarised in Table 7. Table 8 presents the obtained bandwidth for different input powers.

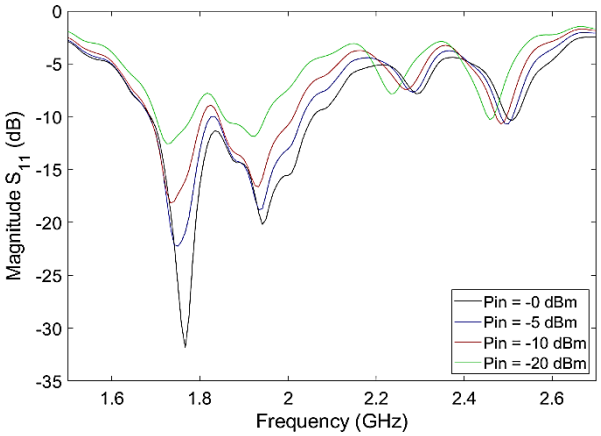

Figure 12. Return loss using different powers.

Table 7. Working frequencies for different input powers.

Power (dBm)	1.ª freq (GHz)	2.ª freq (GHz)	3.ª freq (GHz)	4.ª freq (GHz)
-20	1.73	1.92	2.24	2.45
-10	1.74	1.93	2.27	2.48
-5	1.75	1.94	2.29	2.49
0	1.76	1.94	2.29	2.51

Table 8. Bandwidth using different input powers

	Bandwidth			
Pin (dBm)	1.ª Band for -10dB	2.ª Band for -10dB	3.ª Band for -7dB	4.ª Band for-10dB
-20	100 MHz (1.69-1.79 GHz)	140 MHz (1.84-1.98 GHz)	40 MHz (2.23-2.27 GHz)	20 MHz (2.46-2.48 GHz)
-10	120 MHz (1.69-1.81 GHz)	180 MHz (1.84-2.02 GHz)	40 MHz (2.25-2.29 GHz)	30 MHz (2.47-2.50 GHz)
-5	340 MHz (1.69-2.03 GHz)		40 MHz (2.26-2.30 GHz)	30 MHz (2.48-2.51 GHz)
0	370 MHz (1.69-2.06 GHz)		40 MHz (2.27-2.31 GHz)	30 MHz (2.49-2.52 GHz)

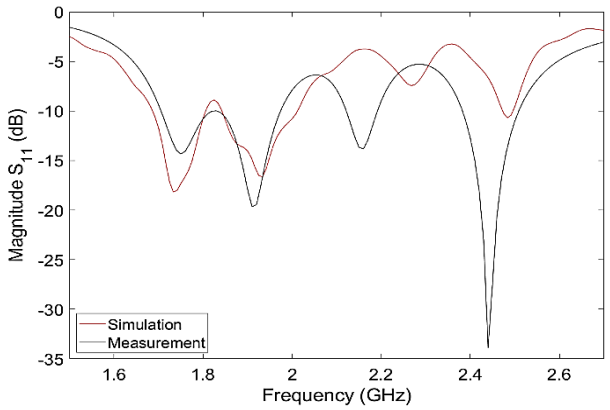

Figure 13. Return loss of simulated and measured rectifier

Table 9. Maximum efficiency results.

	Maximum efficiency (%)	
Frequency (GHz)	Measurement	Simulation
1.75	51.8	37.1
1.85	52.8	46.4
1.95	51.3	50.4
2.15	35.0	45.2
2.45	28.5	39.2

From Figure 13, the most notable differences between simulation and measurement are probably because the ADS library diode does not adequately model the actual behaviour of the device, in addition to the fact that the substrate is simulated with the largest loss tangent given by the manufacturer. On the other hand, the diode decreases its performance with increasing frequency. Table 9 shows the maximum power conversion efficiency results for the device.

4.2. Broadband textile antennas

The joints between the patch, the substrate and the ground plane should not affect the properties of the antenna, therefore adhesive sheets or the use of electrotextiles with an adhesive face are the best options. An alternative technique to join the pieces is sewing, however the seam must be flat and wrinkle-free, which makes flexibility more difficult. Furthermore, a short circuit can be generated between the substrate and the ground plane since the thread contains a small conductivity.

The connection of the SubMiniature Version A (SMA) connector with the antenna is not trivial, because they cannot be soldered on the fabric.

4.2.1. Antenna based on rectangular patches

The prototypes are first implemented with copper tape on the patch, then replaced with conductive fabric (the ground plane is always built with the tape for lack of fabric). Figure 14 shows the constructed prototype with copper tape on the patch. The next step to follow is to build a prototype using conductive cloth on the patch. The manufacture of this antenna is done on the front of a cotton shirt; thus, it is necessary to simulate the shirt and the double-sided adhesive sheets, using the dielectric constants of such materials. When doing this simulation, it was found that the contribution of these elements is minimal because their thickness is much less than that felt, which can be verified mathematically:

$$\mathcal{E}_{eq} = \left(\sum_{n=1}^{N} \frac{t_n}{\mathcal{E}_n}\right)^{-1} \cdot \left(\sum_{n=1}^{N} t_n\right) \tag{28}$$

$$\varepsilon_{eq} = \left(\frac{2.5}{1.12} + \frac{0.3}{1.6} + \frac{0.1}{4}\right)^{-1} (2.5 + 0.3 + 0.1) = 1.18 \tag{29}$$

Where $\mathcal{E}_{eq}$ is the equivalent dielectric constant, t_n and $\mathcal{E}_n$ are the thickness and the dielectric constant of element n.

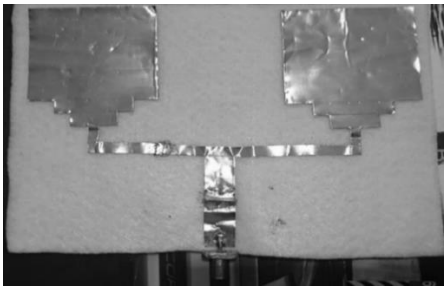

Figure 14. Two elements array antenna made of copper tape.

Figure 15 shows the prototype implemented with conductive fabric. The construction of this antenna is more complex because the transmission lines and the patch are carried out on opposite sides of the shirt, furthermore it is done manually using pencil, ruler and scissor. Joining the elements generates losses since the seam does not completely join them. The idea of putting visible patches on the shirt and hidden transmission lines is for an aesthetic purpose.

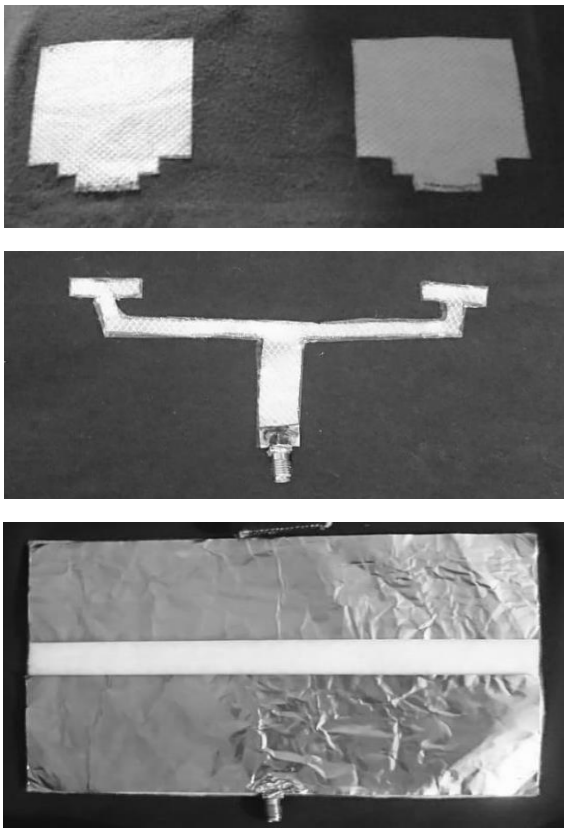

Figure 15. Two elements array antenna made on the T-shirt.

Table 10 shows that the antenna on the T-shirt has a higher bandwidth, but its coupling is the worst, since the reflection coefficient it is very close to -10 dB for the required frequency range.

Table 10. Bandwidth results.

Antenna	Bandwidth for -10 dB (MHz)	Fractional bandwidth (%)
Simulation	1670 - 3110	65
Copper tape	1690 - 3210	62
Conductive fabric	1390 - 3200	78

In figure 16 the antenna on the T-shirt gave more distant results from the designed model, which makes a lot of sense due to the errors introduced in its fabrication (different length and width compared to the design).

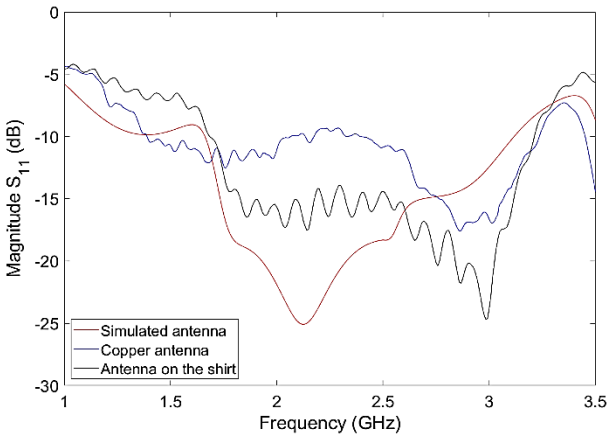

Figure 16. Return loss of simulated and manufactured antennas.

4.2.2. Antenna based on rectangular patches

The prototype implemented with copper tape is presented in Figure 17 and the prototype built on the back of the shirt can be seen in Figure 18. The fabrication of the textile antenna is more complex than the 2-element antenna, due to the greater number of patch connections and transmission lines. These joints cause conduction losses due to the resistance generated. Figure 19 shows that the antenna on the shirt gave more distant results, due to construction errors. Table 11 summarizes the bandwidth results for the collinear antenna.

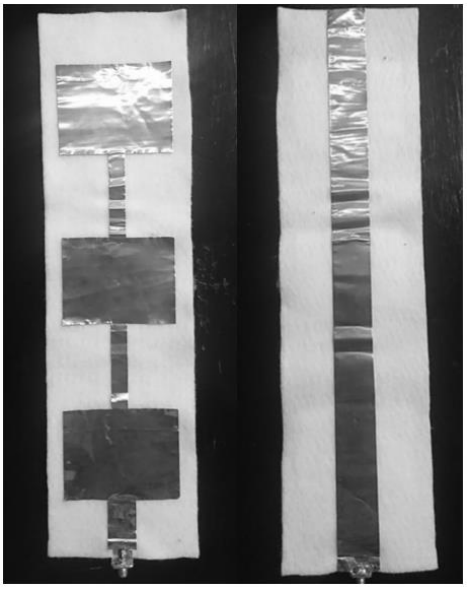

Figure 17. Collinear antenna made of copper tape.

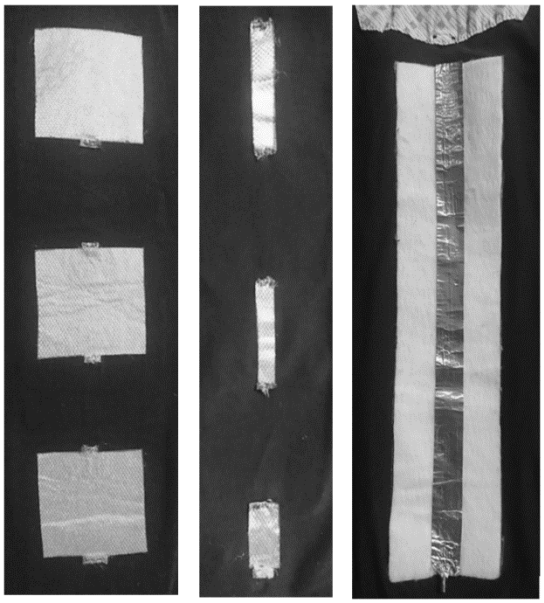

Figure 18. Collinear antenna on the T-shirt.

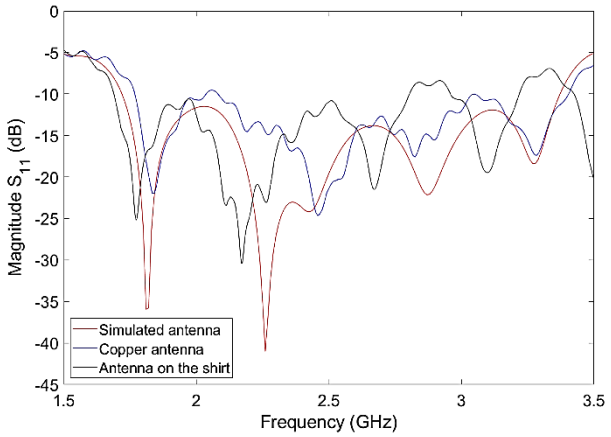

Figure 19. Return loss of simulated and manufactured antennas.

Table 11. Bandwidth results.

Antenna	Bandwidth for -10 dB (MHz)	Fractional Bandwidth (%)
Simulation	1720 - 3370	65
Copper tape	1770 - 3400	63
Conductive fabric	1690 - 3220	62

4.3. Rectenna

For the testing of the system, it is recommended to be close to sources of RF signals, therefore three devices were used: A cell phone, a router and a WiFi repeater. Both antennas were used separately to perform the tests in which the measurement parameter was the output voltage of the rectifier. In the tests carried out with the mobile phone, when establishing a call, voltages above 100 mV were achieved. For tests using the router, voltages between 250 mV and 500 mV were obtained. Finally, when the WiFi repeater was used, voltages between 1 V and 5 V were measured. It is important to emphasize that the variation of the output voltages depends on the proximity of the antenna with the emitting device, on the signal energy at that time and the direction of the antenna pointing to the source.

To test the system in an application, two Light Emitting Diodes (LED) were placed in series at the output and their lighting was observed. The measured output voltage on the diodes was 4.18 V. The power delivered by the rectenna is calculated below:

$$P_o = \frac{V^2}{R} = \frac{(4.18\ V)^2}{(12\ k\Omega)} = 1.46\ mW \tag{30}$$

Table 12 shows how the voltage varies with the distance between the antenna and the emitter using the WiFi repeater.

Table 12. Voltage variation as a function of distance.

	80 cm	50 cm	30 cm	10 cm
Voltage	0.68 V	1.01 V	1.81 V	4.37 V

5. Conclusions

A multi-band rectifier was designed and manufactured to collect energy from the environment, coming from RF signals from four mobile phone bands: 1700, 1800, 1900 and 2100 MHz, as well as from the 2400 MHz WiFi band. The prototype multiplies four times the signal voltage and provides maximum efficiencies around 50% for powers between -5dBm and 0dBm. In this context, two broadband antennas were implemented using microstrip technology. The antennas were fabricated with textile materials using conductive fabric as conductor and felt as substrate to be implemented in clothing. On the front of the T-shirt an antenna was placed based on two rectangular patches fed in parallel, which provided a fractional bandwidth of 70% and gain between 5 dBi and 6.4 dBi for the working frequencies. On the back of the T-shirt, a three-element collinear antenna fed in series was implemented, which provided a fractional bandwidth of 72% and gain between 5 dBi and 7.4 dBi.

The rectenna was tested with signals from mobile networks when establishing a call with a cell phone, the results showed that tens of mV up to 200 mV could be obtained. On the other hand, tests were carried out with a router and a WiFi amplifier to obtain signals with higher powers. In the case of the router, voltages between 300 mV and 400 mV were achieved at a distance of 10 cm. With the WiFi repeater, voltages above 0.5 V were obtained for distances close to 1

meter and voltages close to 4 V for distances around 10 cm. In these tests powers of up to 1.5 mW were achieved. Results show the advantages and potential of this technology if the device is located in an environment with a large amount of RF energy. Wireless devices such as Xbox controls, smart handles, and sensors can be powered using this technology.

Figure 13 shows the reflection coefficient of the rectifier implemented in simulation and the manufactured rectifier. The experimental results of the first two frequency bands (1700 MHz and 1900 MHz) are very close to the results obtained in simulation, for the third frequency band (2200 MHz) there was a difference of 120 MHz between the operating frequency of the manufactured prototype and the design implemented in simulation, finally, for the fourth working frequency (2400 MHz) the difference was 40 MHz. Despite these differences, the results of return loss cover all required frequencies.

Figure 16 shows the return losses of the antennas based on rectangular patches, implemented in simulation, prototype made of copper and the prototype implemented in t-shirt. The results of the simulated antenna and the manufactured prototypes differ a little, which makes a lot of sense due to the errors introduced in its manufacture made manually. However, the return loss of the fabricated prototypes adequately cover all frequencies of interest.

Figure 19 shows the return losses of the collinear antennas, implemented in simulation, prototype made of copper and the prototype implemented in t-shirt. The results of the simulated antenna and the model made of copper are similar, however, the results of the prototype implemented in the t-shirt differ a little from the simulated antenna, which makes a lot of sense due to the errors introduced in its manufacture made manually. Despite this, the return loss of this prototype adequately covers all frequencies of interest.

Finally, energy harvesting from radiofrequency signals has great potential for multiple low power electronic applications, such as IoT devices and wireless sensors. For example, thanks to the possibility of innovating electronic devices without batteries, it allows continuous operation of wireless sensors located in places that could present risks to humans when the battery needs to be replaced, such as in volcanoes, caves, rivers, etc. Another field in which this type of technology could have a great impact is in medicine, since multiple applications could be created to monitor the behavior of the body, for example, monitoring heart rate through pacemakers that do not require battery replacement and in this way the patient does not have to undergo surgeries every so often to replace the battery.

Conflict of interest

The authors have no conflict of interest to declare.

Acknowledgement

The authors wish to acknowledge and thank the Instituto Nacional de Astrofísica Óptica y Electrónica for supporting the development of this paper.

Funding

This work was supported by INAOE.

References

Adami, S. E., Proynov, P., Hilton, G. S., Yang, G., Zhang, C., Zhu, D., ... & Stark, B. H. (2017). A flexible 2.45-GHz power harvesting wristband with net system output from− 24.3 dBm of RF power. *IEEE Transactions on Microwave Theory and Techniques*, *66*(1), 380-395. https://doi.org/10.1109/tmtt.2017.2700299

Agilent Technologies (2005). Agilent HSMS-285x Series Surface Mount Zero Bias Schottky Detector Diodes. Datasheet.

Balanis, C. A. (2016). Antenna theory: Analysis and design (4a ed.). Wiley-Interscience.

Borges, L. M., Barroca, N., Saraiva, H. M., Tavares, J., Gouveia, P. T., Velez, F. J., ... & Balasingham, I. (2014). Design and evaluation of multi-band RF energy harvesting circuits and antennas for WSNs. In *2014 21st International Conference on Telecommunications (ICT)* (pp. 308-312). IEEE. https://doi.org/10.1109/ict.2014.6845129

Cicchetti, R., Miozzi, E., & Testa, O. (2017). Wideband and UWB antennas for wireless applications: A comprehensive review. *International Journal of Antennas and Propagation*, *2017*. https://doi.org/10.1155/2017/2390808

de la Peña Valencia, B. G., & del Castillo Rodíguez, F. D. (2009). Elementos de electrónica. Universidad Nacional Autónoma de México.

Jabbar, H., Song, Y. S., & Jeong, T. T. (2010). RF energy harvesting system and circuits for charging of mobile devices. *IEEE Transactions on Consumer Electronics*, *56*(1), 247-253. https://doi.org/10.1109/tce.2010.5439152

Mutee-Ur-Rehman, Ahmad, W., Qureshi, M. I., & Khan, W. T. (2017). A highly efficient tri band (GSM1800, WiFi2400 and WiFi5000) rectifier for various radio frequency harvesting applications. In *2017 Progress in Electromagnetics Research Symposium-Fall (PIERS-FALL)* (pp. 2039-2044). IEEE. https://doi.org/10.1109/piers-fall.2017.8293473

Naresh, B., Singh, V. K., & Bhargavi, V. (2017). Dual band RF Energy Harvester for Wearable Electronic Technology. In *2017 Third International Conference on Advances in Electrical, Electronics, Information, Communication and Bio-Informatics (AEEICB)* (pp. 274-277). IEEE. https://doi.org/10.1109/aeeicb.2017.7972428

Polivka, M., & Holub, A. (2007). Collinear and coparallel principles in antenna design. In Proceedings of the Progress in Electromagnetics Research Symposium (PIERS'07) (pp. 337-341).

Predella, P., Buxton, J., Schweber, B., & Bryant, J. (1991). Analog Dialogue, vol. 25.

Rhea, R. W. (1994). HF filter design and Computer Simulation. McGraw-Hill.

Rogers Corporation (2018). RT/duroid® 5870 /5880 High Frequency Laminates. Data Sheet.

Salvado, R., Loss, C., Gonçalves, R., & Pinho, P. (2012). Textile materials for the design of wearable antennas: A survey. *Sensors*, *12*(11), 15841-15857. https://doi.org/10.3390/s121115841

Ouyang, Y., & Chappell, W. J. (2008). High frequency properties of electro-textiles for wearable antenna applications. *IEEE Transactions on Antennas and Propagation*, *56*(2), 381-389. https://doi.org/10.1109/tap.2007.915435